Fission of Gold with 112-Mev C^{12} Ions: A Yield-Mass and Charge-Distribution Study*

H. MARSHALL BLANN†
Lawrence Radiation Laboratory, University of California, Berkeley, California
(Received October 4, 1960); revised manuscript received May 12, 1961)

Fission-product cross sections have been measured radiochemically and mass-spectrometrically for gold bombarded with 112-Mev C^{12} ions. Cross sections for 43 nuclides have been measured for elements from nickel to barium. Thirty-six yields are either primary fission-product yields (independent yields) or have been corrected (with less than 25% correction) so as to represent independent yields. The independent yields have been empirically systematized, and a yield-mass curve has been constructed. The yield-mass curve is compared with the yield-mass curves obtained from the fission of bismuth with 22-Mev and 190-Mev deuterons. The yield systematics indicate that the sum of the mass numbers of complementary fission products is 13 ± 1 amu less than that of the compound nucleus, and the sum of the charges of complementary fission products is 2-units less than that of the compound nucleus. By thermodynamic arguments it is shown that the loss of charge was carried by an alpha particle, not by protons.

The most probable charge of the fission products as a function of mass number has been determined empirically and compared with theoretical prediction. The charge-dispersion curve (fraction chain yield vs $Z-Z_p$) may be fitted well by the Gaussian $y=\exp[-(Z-Z_p)^2/0.9]/(0.9\pi)^{\frac{1}{2}}$. Experimental yields on both sides of $Z-Z_p=0$ support the symmetry of the charge-dispersion curve that many workers have assumed.

I. INTRODUCTION

FEW fission-yield investigations have been performed on targets of atomic number less than that of thorium (90). Fairhall and Jensen have bombarded radium with 11-Mev protons and observed three distinct peaks in the mass-yield curve corresponding to the asymmetric and symmetric modes.[1] Fairhall also studied the system Bi^{209} plus 15- and 22-Mev deuterons and observed a single narrow symmetric peak.[2] Fairhall *et al.* found a single narrow symmetric peak for the fission of lead isotopes with 25- to 42-Mev helium ions.[3] Griffioen and Cobble found a symmetric peak for the fission of tantalum and rhenium with helium ions of more than 40 Mev, asymmetric fision becoming relatively more important below 40 Mev.[4] Much less work has been done on the fission of elements lighter than thorium at high excitation energy (greater than 50 Mev). Probably the best-known work in this region is the investigation by Goeckermann and Perlman of the fission of bismuth with 190-Mev deuterons.[5] Unfortunately, when the energy of the bombarding particle exceeds about 50 Mev per nucleon, the compound-nucleus model becomes invalid as direct interactions take place; nucleon-nucleon collisions cause cascade particles to be knocked out of the nucleus, resulting in a large number of excited nuclear species having a broad spectrum of excitation energy.[6]

The Berkeley heavy-ion linear accelerator (Hilac) provides a means of attaining high excitation energy in a single compound nucleus. Here we are considering only compound-nucleus formation; stripping reactions are ignored, since they should not contribute significantly to the fission cross section of gold; e.g., $\sigma_F/\sigma_R=10^{-4}$ for 40-Mev alpha particles on gold, whereas for 112-Mev C^{12} ions on gold σ_F/σ_R is of the order of magnitude of 1 (where σ_F/σ_R is the ratio of fission cross section to total reaction cross section).[7] Projectiles ranging from He^3 to A^{40} are accelerated to an energy of 10 Mev per nucleon, far too low for the nucleon-nucleon cascade process. Gold was chosen as a target because it is monoisotopic and high-purity foils are available. Bombardments have been performed with C^{12} ions of up to 112 Mev. The predicted compound nucleus is At^{209}, with about 89 Mev of excitation. Such systems formed through heavy-ion bombardment have very high angular momenta; the average predicted for the above case is 40 units.[8] With a compound system not preceded by cascade, the mass distribution is more meaningful, and in particular the charge distribution has far more significance than that resulting from proton bombardment at the same energy.

Many workers have investigated the charge distribution in fission. The rules of the game usually have been to measure independent and partial chain fission yields and then to determine by trial and error which of several empirical rules gives the best correlation of the results. ("Independent yield" as used in this work refers to the yield of an isotope from the fission process, and does not include contributions to that yield from β^+, β^-, or electron-capture decay of other isotopes in the same mass chain.) It is understood that there is no reason why any simple rule must explain the experimental results in the complex process of nuclear fission. None-

* This work was performed under the auspices of the U. S. Atomic Energy Commission.
† Present address: University of Rochester, Rochester, New York.
[1] R. C. Jensen and A. W. Fairhall, Phys. Rev. **109**, 942 (1958).
[2] A. W. Fairhall, Phys. Rev. **102**, 1335 (1956).
[3] A. W. Fairhall, R. C. Jensen, and E. F. Neuzil, *Proceedings of the Second United Nations International Conference on the Peaceful Use of Atomic Energy, Geneva, 1958* (United Nations, Geneva, 1958), Vol. 15, p. 452.
[4] R. D. Griffioen, thesis, Purdue University, 1960 (unpublished).
[5] R. H. Goeckermann and I. Perlman, Phys. Rev. **73**, 1127 (1948).
[6] R. Serber, Phys. Rev. **72**, 1114 (1974).
[7] I. Halpern, Ann. Rev. Nuclear Sci. **9**, 245 (1959).
[8] T. Darrah Thomas, Phys. Rev. **116**, 703 (1959).

theless, by learning more about the primary distribution of charge in fission, we can gain additional insight into the nature of the fission processes and the properties of nuclear forces.

II. EXPERIMENTAL PROCEDURE

A. The Target and Irradiations

1. The Target

For radiochemical studies the targets consisted of sheets of 0.1-mil gold. The actual arrangement in the target holder was a stack consisting of two 0.7-mil aluminum foils followed by the 0.1-mil gold foil, which was in turn followed by another 0.7-mil aluminum foil. The first aluminum foil served as a vacuum seal for the target holder; the other two aluminum foils sandwiched the gold target foil and served as catcher foils for the recoiling fission products. In all runs in which absolute cross sections were to be determined an additional 0.25-mil aluminum foil ("crud foil") was placed well in front of the target. The purpose of this foil was to strip fully the carbon ions of electrons. It was important to know the charge state of the carbon ions, since they were all stopped by the target holders, which served as their own Faraday cups.

A mass spectrometer was used to measure the relative yields of fission-produced isotopes of cesium and strontium. The target used for mass spectrometry consisted of a 1-mil aluminum beam-degrader foil followed by a 0.5-mil gold foil. No additional catcher foil was used. When thinner gold targets were used, the number of cesium and strontium atoms formed was insufficient for mass spectrometry.

Spectrographic analysis (optical) of the 0.1- and 0.5-mil gold foils set an upper limit of 0.1% for heavy elements. The aluminum foils were 99.5% pure.

2. Radiation Detection

Beta radiation was counted by use of an end-window proportional counter. The detector response was calibrated by standardization with varying thicknesses of various β emitters, as described by Bayhurst and Prestwood.[9] Efficiency curves were determined for all shelf positions used. All β-decay curves of more than two components were resolved by use of the "Frenic" IBM-704 least-squares program (a Los Alamos program).

Gamma spectra were observed by using a 100-channel pulse-height analyzer (PENCO) with 3×3-in. and 1.5×1-in. thallium-activated NaI crystals. Crystal efficiencies were determined experimentally by using Na^{22} and Cs^{137} samples of known disintegration rate. These values were found to be in good agreement with published values; the published curves then were used.[10,11]

B. Cross Sections and Results

The cross sections for all nuclides measured are listed in column 2 of Table I. If the cross sections have been corrected so as to represent independent yields, these are listed in column 3. The method of obtaining the numbers in columns 3 and 4 is discussed in the next section. The other column headings are self-explanatory. The limits of errors quoted are felt to be reasonable; in most cases ±20% has been estimated for the absolute errors between nuclides of different elements. The relative errors for isotopes of a fixed Z are much smaller. If there was difficulty in resolving decay components (as in the gamma-spectra resolution resulting from decay of iodine isotopes), or if the half-life was somewhat uncertain (as with Y^{94}), a larger absolute error has been indicated. The results of the lower-energy bombardments are listed at the end of the table. For the yields of niobium isotopes from the target bombarded with 76-Mev C^{12} ions, no uncertainties are listed because an unidentified contamination made decay-curve resolution very uncertain. The yttrium cross sections from the lower-energy bombardments have less than 20% errors indicated. The smaller error estimation has been chosen because these yttrium cross sections are compared only with the yttrium cross sections from the 112-Mev bombardments and not with cross sections of other nuclides.

III. DISCUSSION

A. Correlation of Results

In most fission-product studies the fission fragments are very neutron-rich. Thus, chain yields are easily measured, but it is difficult to measure a large number of independent yields. In this work, the neutron-deficient properties of the probable compound nucleus (At^{209}) and the high excitation energy (89 Mev) made the reverse true. The fission products varied from slightly neutron-rich to neutron-deficient, and it was very difficult to measure total chain yields, since a stable isotope usually comprised a significant part of the total chain yield. The term "chain yield" is used in a rather loose sense in this work; it is used to mean the cumulative isobaric yield, even though the "chain" may contain β^-, β^+, electron capture, and stable isotopes. It is necessary to correlate the data in some way such that the yields of stable or unmeasured isotopes may be estimated.

It was decided to attempt construction of the three-dimensional yield surface Z vs A vs cross section (σ). Several independent yields were measured experi-

[9] B. P. Bayhurst and R. J. Prestwood, Nucleonics **17**, 82 (1959).

[10] J. M. Hollander and M. Kalkstein, University of California Radiation Laboratory Report UCRL-2764, 1954 (unpublished).

[11] R. L. Heath, Atomic Energy Commission Research and Development Report IDO-16408, 1957 (unpublished).

mentally for each of several elements. Thus, each of these represented the variation of yield with mass number for fixed Z, that is, the two-dimensional σ vs A function for fixed Z. These isotopic yield functions formed the slabs used to construct the three-dimensional yield surface. If the points denoting σ vs A for some Z are connected, they define a curve. This curve is either the same for all Z, or different. If it is different, it is not unreasonable to guess that the greatest difference will show up between a Z in the "symmetric" fission region and a Z in the "asymmetric" fission region. Therefore, cross sections for formation of yttrium and cesium isotopes were measured very carefully (see Appendix) and compared (Fig. 1) to determine whether the curve shape was dependent on or independent of Z. (The yields of cesium isotopes were corrected slightly so as to represent independent yields; a small correction was also applied to correct for the yield-distribution broadening because of the 0.5-mil foil used.) Fortuitously, Fig. 1 shows no drastic Z dependence. Therefore, a first rough three-dimensional construction was made, using the shape determined by the two slabs due to yttrium and cesium. In order to interpolate missing slabs it was necessary to know the mass number (not necessarily integral) at which the maximum of each yield vs A curve occurred, and the cross section at this maximum. The previously determined distribution about this maximum (Fig. 1) then determined all yields for the element. Finding these maxima required the major assumptions of the data correlation.

It was assumed that the variation, as a function of Z, of maximum cross section and of the A at which that maximum occurred were both smooth functions—that is, that interpolation was valid. For elements for which several independent yields were measured, the curve for cross section vs A was drawn through these points,

TABLE I. Results (half-lives and decay schemes from reference 12 unless otherwise noted).

Nuclide	Cross section (mb) Measured	Corrected to independent yield	Fractional chain yield[a]	Radiation detected	Assumed radiation abundance (particles per disintegration)	Number of determinations	Half-life used
With 112-Mev C^{12} ions							
Ni^{65}	1.36±0.14			β^-		5	2.56 hr
Ni^{66}	1.25±0.13	1.0±0.2	0.50	β^-	2	5	54.6 hr
As^{74}	0.47±0.10	0.47±0.10	0.054	β^+,β^-	0.62	1	17.5 days
As^{76}	2.8±1.4			β^-		1	26.4 hr
	3.7±0.8	3.7±0.8	0.31	560-kev γ	0.36 γ/dis		26.4 hr
As^{77}	10.0±2			β^-	1	1	38.7 hr
As^{78}	5.6±1			β^-	1	1	90 min
Br^{80}	~0						
Br^{80m}	5.4±1.1	5.4±1.1	0.27	Br^{80} β^-,β^+	0.95	3	4.4 hr
Br^{82}	12±2.4	12±2.4	0.46	β^-	1	3	35.9 hr
Br^{83}	17.5±3.5			β^-	1	3	2.3 hr
Br^{84m}	5.5±1.1	7±1.5	0.23	β^-	1	1	6.0 min
Br^{84}	2±0.4			β^-	1	1	32 min
Sr^{89}	38.8±8.8			β^-	1	2	50.5 days
Sr^{90}	33±5			(Mass spec. ratio Sr^{89}/Sr^{90})		2	
Sr^{91}	20.4±3	18±3	0.36	β^-	1	2	9.67 hr
Y^{90}	16.3±3	16.3±3	0.34	β^-	1	4	64.2 hr
Y^{91}	24±5	24±5	0.48	β^-	1	4	57.5 days
Y^{92}	25.7±5	25.7±5	0.49	β^-	1	4	3.60 hr
Y^{93}	24.5±5	20.5±5	0.38	β^-	1	4	10.4 hr
Y^{94b}	12.8±3.6	11.0±3.6	0.20	β^-	1	4	16.5 min, 20 min
Y^{95}	4.4±2.2	4.4±2.2	0.077	β^-	1	1	10.5 min
Zr^{95}	34±7	30±7	0.53	β^-	1	1	65 days
Zr^{97}	11.6±2	11.6±2	0.19	β^-	2	1	17 hr
	11.5±2			747+665-kev γ's	2	1	
Nb^{95}	17±3	17±3	0.30	765-kev γ	1	2	35 days
Nb^{96}	29±6	29±6	0.50	β^-	1	2	23.3 hr
Nb^{97}	38±8	37±8	0.59	β^-	1	2	72.1 min
Nb^{98c}	24±6	20±6	0.33	β^-	1	2	51.5 min
Mo^{99}	45±10			β^-	1	6	66 hr
Ag^{111}	17±3	16.4±3	0.53	β^-	1	1	7.6 days
Ag^{112}	10.8±2	10.5±2	0.37	β^-	1	1	3.20 hr
Ag^{113}	7.6±1.5	6.9±1.5	0.26	β^-	1	1	5.3 hr
Ag^{115}	0.92±0.20	0.8±0.2	0.035	β^-	1	1	21.1 min
I^{121}	0.04±0.01	0.04±0.01	0.0035	210-kev γ	0.92	2	2.0 hr
I^{123}	0.44±0.12	0.42±0.12	0.049	160-kev γ	0.83	2	13.0 hr
I^{124d}	1.20±0.30	1.20±0.30	0.16	600-kev γ	0.64	2	4.2 days
I^{125}	3.2±0.6	3.2±0.6	0.50	Te K x rays	1.39	1	60 days
I^{126}	3.1±0.6	3.1±0.6	0.62	380-kev γ	0.33	2	13.3 days
I^{126}	3.1			480-kev γ	0.05		
I^{126}	3.2			650-kev γ	0.33		
I^{128}	1.0±0.3	1.0±0.3	0.27	460-kev γ	0.17	2	25.0 min

TABLE I (*continued*).

Nuclide	Cross section (mb) Measured	Corrected to independent yield	Fractional chain yield[a]	Radiation detected	Assumed radiation abundance (particles per disintegration)	Number of determinations	Half-life used
With 112-Mev C^{12} ions							
I^{130}	$\geqslant 0.077 \pm 0.02$	$\geqslant 0.088 \pm 0.02$	$\geqslant 0.035$	410-kev γ	$\leqslant 0.30$	1	12.6 hr
I^{130}	$\geqslant 0.087$			530-kev γ	$\leqslant 1.00$		
I^{130}	$\geqslant 0.100$			660-kev γ	$\leqslant 0.90$		
Cs^{127}	0.079 ± 0.02	0.075 ± 0.02	0.017	mass spec, γ		1	6.3 hr
Cs^{129}	0.6 ± 0.12	0.54 ± 0.12	0.18	380-kev γ mass spec	$\leqslant 1.00$	1	30.7 hr
Cs^{131}	1.1 ± 0.22	1.1 ± 0.22	0.54	mass spec		1	9.6 days
Cs^{132}	0.9 ± 0.18	0.9 ± 0.18	0.53	670-kev γ mass spec	0.98	1	6.2 days
Cs^{135}[e]	0.090 ± 0.018	0.086 ± 0.018	0.096	mass spec		1	3×10^6 yr
Ba^{131}	0.16 ± 0.04	0.15 ± 0.04	0.075	Cs and Xe K x rays	0.94 0.73	1	11.5 days
With 95-Mev C^{12} ions							
Y^{90}	8.9 ± 0.9	8.9 ± 0.9		β^-	1	1	64.2 hr
Y^{91}	17.5 ± 2	17.5 ± 2		β^-	1	1	57.5 days
Y^{92}	23 ± 2	22 ± 2		β^-	1	1	3.6 hr
Y^{93}	27 ± 3			β^-	1	1	10.5 hr
Y^{94}[b]	21 ± 4			β^-	1	1	19.5 min
Nb^{95}	9.4 ± 2	9.4 ± 2		765-kev γ	1	1	35 days
Nb^{96}	16.0 ± 3	16 ± 3		β^-	1	1	23 hr
Nb^{97}	32 ± 6	32 ± 6		β^-	1	1	72.5 min
Nb^{98}[c]	15 ± 3			β^-	1	1	51.5 min
With 76-Mev C^{12} ions							
Y^{90}	1.05 ± 0.1	1.05 ± 0.1		β^-	1	1	64.2 hr
Y^{91}	3.00 ± 0.3	3.00 ± 0.3		β^-	1	1	57.5 days
Y^{92}	5.30 ± 0.5	4.9 ± 0.7		β^-	1	1	3.6 hr
Y^{93}	8.7 ± 0.9			β^-	1	1	10.5 hr
Y^{94}	8.4 ± 1.6			β^-	1	1	19.5 min
Nb^{95}	$\leqslant 1.3$			765-kev γ	1	1	35 days
Nb^{96}	9.7			β^-	1	1	23 hr
Nb^{97+98}	18			β^-	1	1	$\approx$70 min

[a] Independent yield ÷ total isobaric yield.
[b] From reference 13.
[c] From reference 14.
[d] From reference 15.
[e] From reference 16.

fixing $A_{\max}$ and $\sigma_{\max}$. These were each plotted vs Z; the plot of $\sigma_{\max}$ vs Z is shown in Fig. 2, with the smooth curve drawn through these points. Similarly a plot of $A_{\max}$ vs Z was used to interpolate $A_{\max}$. From these curves it was possible to construct the three-dimensional surface represented in Fig. 3.

The first construction of Fig. 3 was used to correct some additional cumulative yields so as to represent independent yields. This was done when the correction did not exceed 25% of the measured cumulative yield. Thus, cross sections of comparable size were not subtracted unless both were experimentally measured. This was the method used to get entries in column 3 of Table I. The shape of the curve for isotopic yield vs A was redetermined by using the directly measured and corrected independent yields of bromine, yttrium, niobium, silver, iodine, and cesium. These yields seemed consistent with the curve $y=\exp[-(A-A_Z)^2/6]/(6\pi)^{\frac{1}{2}}$ = fraction isotopic yield (where A_Z is the most probable mass number for the atomic number "Z"), as may be seen in Fig. 4. The curve of Fig. 4 replaced the curve of Fig. 1 for final construction of the three-dimensional surface of Fig. 3.

Isobaric slices of Fig. 3 were summed to obtain the yield-mass curve of Fig. 5. Where experimental values were available, these were used. Mass values for construction of Fig. 5 were in general selected where experimental yields were available. These slices were also used to determine Z_p for various A. The distribution of fraction chain yield vs the $Z-Z_p$ so determined is shown in Fig. 6. The Z_p determined in this manner is estimated to be correct to ± 0.2 charge unit, and the smooth correlation of the charge-dispersion curve is consistent with this estimate. The solid curve of Fig. 6 is the Gaussian, $y=\exp[-(Z-Z_p)^2/0.9]/(0.9\pi)^{\frac{1}{2}}$ = fraction chain yield.

The question arises whether the functions constructed from Fig. 3 are unique (within the uncertainties quoted) or arise as a consequence of the assumptions used in the construction.

We feel that the yield-mass and charge-dispersion curves are, within the quoted uncertainties, unique.

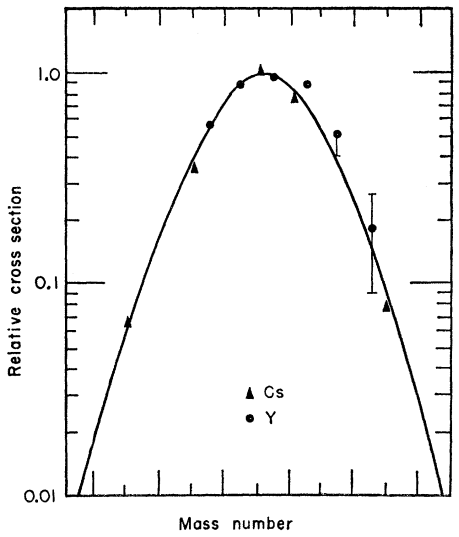

FIG. 1. Comparison of Y and Cs cross section vs A distributions. (The abscissa has 1 mass unit per division.)

The reasons are that the yield-mass curve is drawn through points representing mainly measured yields. The sums of measured yields are shown in Fig. 5 as triangles, whereas circles represent sums of measured plus estimated yields. Figure 4 is good justification for assuming an isotopic yield shape independent of Z, and placement of curves in construction of Fig. 3 was further aided by the requirement that estimated independent yields sum to measured partial chain yields. Essentially the same charge dispersion curve may be obtained from the three independent yields of Y^{95}, Zr^{95}, and Nb^{95}, assuming only that the shape is Gaussian.

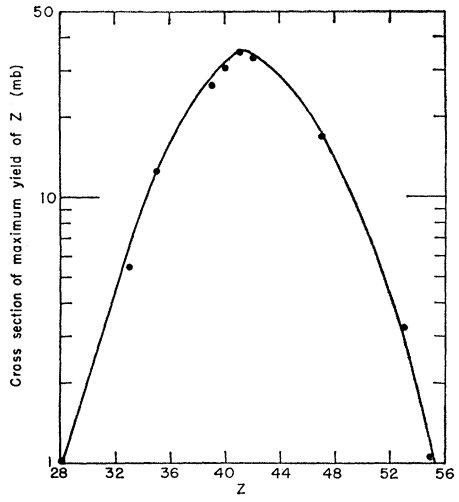

FIG. 2. Cross section of maximum isotopic yield vs Z. This curve was also used to determine the number of charged particles emitted.

[12] D. Strominger, J. M. Hollander, and G. T. Seaborg, Revs. Modern Phys. **30**, 585 (1958).

This assumption has been fairly well justified experimentally in other systems.[17]

B. Yield-Mass Curve

The yield-mass curve (Fig. 7) is symmetric about mass No. 98 and is 27 mass No. wide at half maximum. The yield-mass curves measured for the fission of bismuth with 22-Mev deuterons and for bismuth with 190-Mev deuterons are shown in Fig. 7 as broken lines.[2,5] Fairhall's work (bismuth+22-Mev d) shows a symmetric peak centered about mass No. 103.5 and having a 17-unit width at half maximum. The work of Goeckermann and Perlman (Bi^{209}+190-Mev d) shows a symmetric distribution centered about mass No. 99. The comparison shows a narrower peak in the low-energy bombardment than in the higher-energy bombardments, which could be attributable to lower excitation in the fissioning nucleus, less variety of fissioning

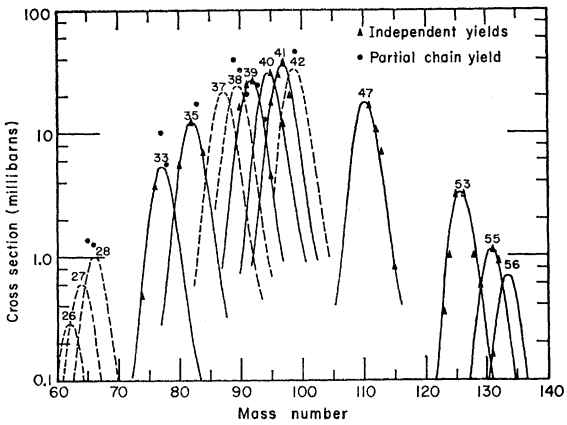

FIG. 3. "Isotopic shape" of Fig. 1 normalized to measured independent yields (solid lines). Several interpolated curves are shown as broken lines. The atomic number corresponding to each curve is written directly above the curve.

nuclei, or both. Comparison of the two high-energy peaks shows that the system bismuth+190-Mev d gives a fissioning nucleus with approximately the same average excitation energy as the system Au^{197}+112-Mev C^{12}. This follows from the observation that both peaks are in nearly the same position as a function of mass number. The greater width of the peak resulting from the fission of bismuth with 190-Mev deuterons is most likely attributable to greater spread of excitation energies about the average than for the $Au^{197}+C^{12}$

[13] Kurt Wolfsberg, thesis, Department of Chemistry, Washington University, 1959 (unpublished), p. 67.
[14] David E. Troutner, thesis, Washington University, August, 1959 (unpublished).
[15] A. C. G. Mitchell, Jose O. Juliano, Chas. B. Creager, and C. W. Kocher, Phys. Rev. **113**, 628 (1959).
[16] James R. Grover, thesis, University of California Radiation Laboratory Report UCRL-3932, 1957 (unpublished), pp. 49–50.
[17] David Nethaway, thesis, Washington University, September, 1959 (unpublished).

system, as well as to a greater variety of fissioning nuclei due to nucleon-nucleon cascade reactions. It is at present impossible to make any assessments, solely from the experimental data of this work, of the effect of high angular momentum on the fission process.

The cross section for fission found in this work was 0.9 ± 0.3 barn, which may be compared to a predicted compound-nucleus cross section of 1.9 barns.[8] Goeckermann and Perlman found a 0.2-barn cross section for fission of bismuth with 190-Mev deuterons, and Fairhall found a fission cross section of about 10^{-5} barn for bismuth plus 22-Mev deuterons.[2,5]

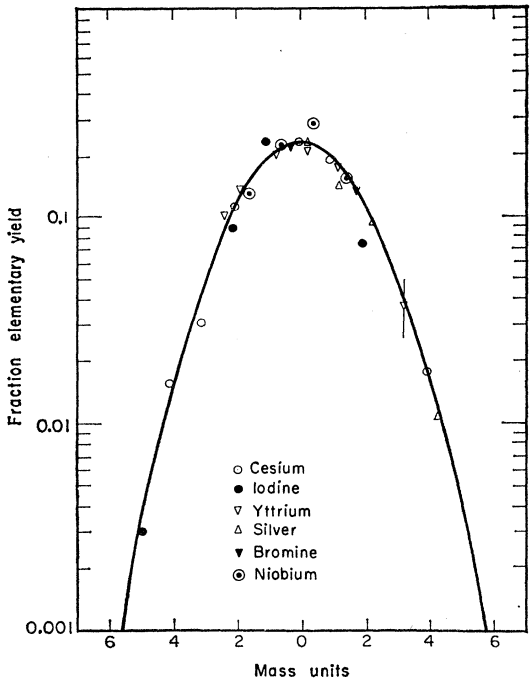

FIG. 4. Final isotopic yield curve used to construct Fig. 3. (The abscissa gives $A-Az$.)

C. Charged-Particle Emission

How many nucleons were emitted in the fission act? An estimate of the total nucleon emission may be obtained by "folding" the yield-mass curve. Such folding is accomplished by summing mass numbers having the same yield, as read from Fig. 5. These mass numbers may be said to be yield-complementary. Masses of complementary fragments so defined summed to 196 amu, 13 less than the 209 of the assumed compound nucleus. Similarly, by folding the yield-charge curve (Fig. 2), one finds the peak at $Z=41.5$. The uncertainty here is $\approx\pm0.5$ charge units in the sum. Thus, the sum of the charges of complementary fragments is 83 ± 0.5, two less than the 85 of the compound nucleus. One may conclude that in the average fission process there were 13 ± 1 nucleons emitted, 2 ± 0.5 of them being charged particles.

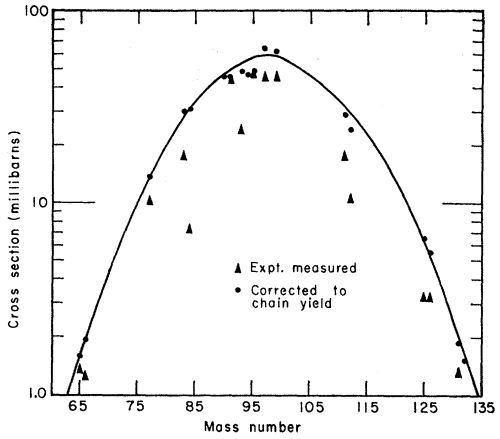

FIG. 5. Yield-mass distribution for fission of Au^{197} with 112-Mev C^{12} ions.

Were the charged particles emitted as protons or as an alpha particle? An answer to this question may be obtained from energy-balance considerations. Consider Table II. Mass values for Table II were taken from the mass tabulation by Cameron, with the exception of mass-excess values for ${}_6C^{12}$, ${}_2He^4$, ${}_0n^1$, and ${}_1H^1$, which were taken from the *G. E. Chart of the Nuclides*.[18,19] As may be seen from the tabulation, the 28-Mev binding energy of the alpha particle is necessary to give a

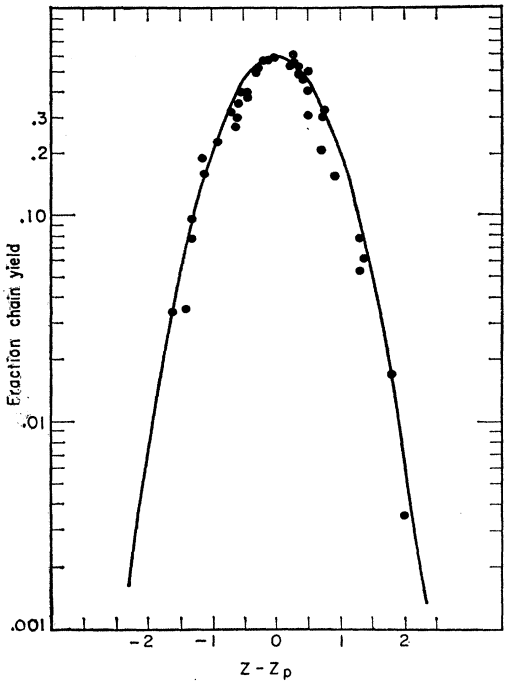

FIG. 6. Charge-dispersion curve $Au^{197}(C^{12},f)$.

[18] A. G. W. Cameron, Atomic Energy of Canada Limited Report AECL-433 CRP-690, 1957 (unpublished), Appendix.
[19] G. Friedlander and M. Perlman, *G. E. Chart of the Nuclides, 1956* (revised by Stehn and Clancy).

TABLE II. Comparison of two possible modes of nucleon evaporation for $_{85}At^{209}$ excited to 89 Mev (c.m.).

	Assumed final products (most probable) $_{41}Nb^{98}+_{42}Mo^{98}+11n+2p$	$_{41}Nb^{98}+_{42}Mo^{98}+9n+\alpha$
Observed kinetic energy (c.m.) of fission fragments (Mev)[a]	144	144
Energy available for kinetic energy of n, p, or α, or for γ emission (Mev)	8	36
Minimum expected kinetic energy of neutrons (Mev)[b]	22	18
Minimum expected total kinetic energy of charged particles (Mev)[c]	18	18
Minimum expected total kinetic energy of neutrons plus charged particles (Mev)	40	36
Comparison with available energy	Inconsistent	Consistent

[a] G. E. Gordon, A. E. Larsh, T. Sikkeland, and G. T. Seaborg, Phys. Rev. **120**, 1341 (1960).
[b] Based on $U^{235}(n,f)$ neutron energy measurements, and V. F. Apalin, U. P. Dobrynin, V. P. Zakharova, I. E. Kutikov, and L. A. Mikaélyan, *The Number of Neutrons Emitted by Individual Fragments in the Fission of U^{235}* Atomic Energy USSR, Jan. 1960, pp. 15–22. Atomnaya Energiya **7**, 375 (1959) [translations: Soviet J. Atomic Energy (Consultants, Bureau, New York) **7**, 853 (1961); Reactor Science (J. Nuclear Energy: Part A) **13**, 86 (1960)].
[c] Calculated from Coulomb barrier considerations; see also Harold C. Britt and Arthur R. Quinton, Phys. Rev. **120**, 1768 (1960).

balance between the energy available for nucleon kinetic energy and the energy required. One would expect 3 to 4 Mev of energy to be lost owing to γ emission.[7] That this energy is apparently not available may be attributed to the one-neutron uncertainty (one less neutron lost would make an additional 8 Mev available), or to experimental error in the 144-Mev value used for kinetic energy of the fission fragments,

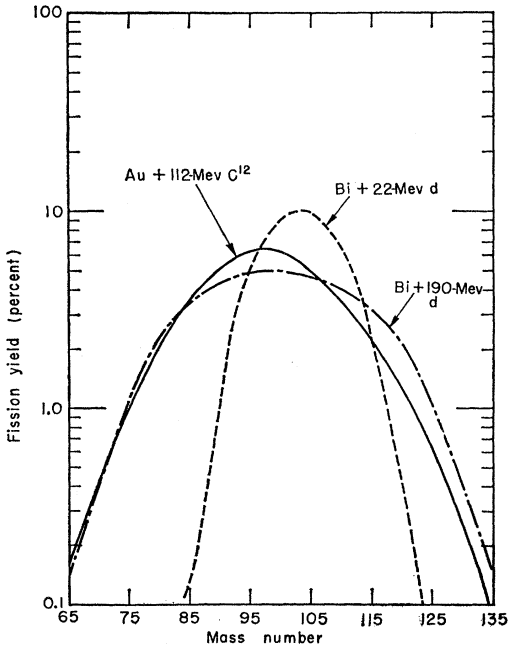

FIG. 7. Several yield-mass curves in the bismuth region.

or both. Actually α-particle emission from the system gold+160-Mev O^{16} ions has been seen by Anderson *et al.*[20] Preliminary results indicate that the average kinetic energy of the emitted α particles is 18 Mev in the center-of-mass system.

D. Charge Distribution

It has been stated that the dispersion of charge about the most probable value (Fig. 6) may be described by a curve $y=\exp[-(Z-Z_p)^2/c]/(\pi c)^{\frac{1}{2}}$, where c has the value 0.9. Actually values of 0.9 ± 0.1 for c are within the experimental uncertainties. This curve is essentially the same as that found in the thermal neutron fission of uranium.[17] One might wonder why this curve is not broader, since the excitation energy is higher than in thermal-neutron-induced fission of U^{235}. However, there is no *a priori* reason why these systems should be comparable; the features of fission around bismuth are known to be entirely different from those around uranium. It is not even known whether Γ_f/Γ_n is large or small for a highly excited At^{209} nucleus.

The variation of Z_p with A is of interest. Several empirical rules to estimate this variation have been suggested.[5,21] Present, and later Fong, offered a theoretical method for predicting Z_p as a function of A.[22,23] Present assumed a model of two tangent spheres at scission, and minimized the potential energy of the system with respect to Coulomb and symmetry energies. The predictions of this theory of Present (as formulated by Swiatecki using constants due to Green) are shown in Fig. 8.[24,25] Also shown in Fig. 8 is a prediction by the so-called "CCR" rule (where the most probable Z/A ratio in a fragment is assumed to be the same as in the fissioning nucleus less neutrons, i.e., 83/196) and a prediction by the ECD or equal-chain-length rule. The Z_A of Grummitt and Milton were used in these calculations.[26]

The smooth curve of Fig. 7 was used to estimate Z_p according to the method suggested originally by Wahl.[27] Fraction chain yields were forced onto the smooth curve, and $Z-Z_p$ (hence Z_p) was read from the intersection of the experimental fraction chain yield value with the charge dispersion curve. The points plotted in Fig. 8 are shown with an uncertainty of ±0.2 charge unit. Evidently Present's theoretical treatment is worth

[20] C. E. Anderson, A. R. Quinton, and W. J. Knox (Yale University), preliminary results (from private communication with W. J. Knox, May, 1960).
[21] L. D. Glendenin, C. D. Coryell, and R. R. Edwards, *Radiochemical Studies: The Fission Products* (McGraw-Hill Book Company, Inc., New York, 1951), Paper No. 52, National Nuclear Energy Series, Plutonium Project Record, Vol. 9, Div. IV.
[22] R. D. Present, Phys. Rev. **72**, 7 (1947).
[23] Peter Fong, Phys. Rev. **102**, 434 (1956).
[24] W. J. Swiatecki, Lawrence Radiation Laboratory (private communication).
[25] A. E. S. Green, Phys. Rev. **72**, 7 (1947).
[26] W. E. Grummit and Gwen M. Milton, Atomic Energy of Canada Limited Report AECL-453 CRC-694, 1957 (unpublished).
[27] A. C. Wahl, J. Inorg. of Nuclear Chem. **6**, 263 (1958).

additional investigation, since it predicts the experimental trend quite nicely.

ACKNOWLEDGMENTS

I wish to express my sincere gratitude to Dr. John M. Alexander, whose interest and direction made the completion of this work possible.

Thanks are due Dr. T. Darrah Thomas for suggesting this study.

I further wish to express my appreciation to Dr. Maynard Michel for the mass-spectrometric analysis and to the Hilac crew for the irradiations.

APPENDIX

Chemistry

All chemical procedures employed in this work may be found in the literature. The compilations used were those of Coryell and Sugarman and the Los Alamos Scientific Laboratory Reports.[28,29] In addition, some solvent extraction procedures were used for separation of yttrium and niobium from other fission products.[30,31]

Nuclides Observed

Nickel

The decay curves obtained by proportional counting always showed two components which were easily resolved graphically. The components represented half-lives of 2.56 hr, corresponding to Ni^{65}, and 54 hr, corresponding to Ni^{66} in equilibrium with its 5.1-min Cu^{66} daughter.

Arsenic

End-window proportional counting gave a decay curve that was resolved, through the use of the IBM-704 Frenic least-squares program, into four components having half-lives of 17.5 days (As^{74}), 39 hr (As^{77}), 26.7 hr (As^{76}), and 90 min (As^{78}).[32] Because the 26.7-hr component was less abundant than the 39-hr group, and because the half-lives were not well separated, resolution of the 26.7-hr component had a large standard deviation associated with it. Therefore, the 26.7-hr As^{76} γ radiation was also observed on the 3×3-inch NaI crystal on the 100-channel pulse-height analyzer.

Bromine

In the long bombardments (1 to 2 hr) three components were observed in the β-decay curves, corresponding to the isotopes with half-lives of 2.3 hr (Br^{83}), 4.4 hr (Br^{80m}), and 35.9 hr (Br^{82}). In a 3.00-min bombardment components of 6.00 min (Br^{84m}), 32 min (Br^{84}), 2.3 hr (Br^{83}), 4.4 hr (Br^{80m}), and 35.9 hr (Br^{82}) were observed. All bromine decay curves were analyzed through the use of the IBM least-squares program. Although the Br^{80} β^- activity of 18-min half-life was put into the guessed decay curve for the IBM least-squares program, the least-squares program would not converge promptly; rather, it showed the 18-min activity at the end of the bombardment as zero counts/min.

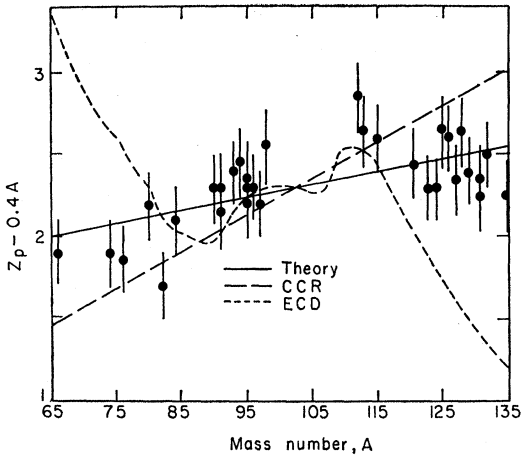

FIG. 8. Variation of most probable charge with mass No. as measured experimentally, as predicted by the theory of Present, and as calculated by empirical rules.

Strontium

The ratio of the yield of Sr^{89} to that of Sr^{90} was determined by use of the mass spectrometer. Strontium-89 and Sr^{91} yields were determined radio-chemically by using the proportional counter. Two-component decay curves resulted which were easily resolved graphically. Twenty hours elapsed after the end of the irradiation before strontium oxalate was precipitated. Several yttrium hydroxide precipitations were performed just prior to the precipitation of the strontium to remove Y^{91} and Y^{92}. The 20-hr delay permitted 80% of the Sr^{91} to decay to Y^{91}, as well as removing the Sr^{92}-Y^{92} pair. Yttrium-91 has a 58-day half-life and would appear as Sr^{89} (50.5-day half-life) in the decay-curve analysis. A small correction was applied to the Sr^{89} disintegration rate for the Y^{91} that was present. This method was quite accurate; the correction was very small.

Yttrium

The proportional counter was used to count β^- particles from the decay of yttrium isotopes from four different bombardments of from 5.00 min to 2 hr. The yttrium fraction from the 5.00-min bombardment showed β-decay components corresponding to half-lives

[28] *Radiochemical Studies: The Fission Products*, edited by C. D. Coryell and N. Sugarman, see reference 24, Book 3, Paper No. 277, p. 1623.

[29] Collected Radiochemical Procedures, Los Alamos Scientific Laboratory Report LA-1721, 1956 (unpublished), p. Ni 1.

[30] H. G. Hicks and R. S. Gilbert, Anal. Chem. **26**, 1205 (1954).

[31] D. F. Peppard, J. P. Faris, P. R. Gray, and G. W. Mason, J. Phys. Chem. **57**, 294 (1953).

[32] For a description of the least-squares program see G. R. Keepin, T. F. Wimett, and R. K. Zeigler, J. Nuclear Energy **6**, 1 (1957).

of about 16 min, 50 min (Y^{91m}), 3.6 hr (Y^{92}), 10.5 hr (Y^{93}), 64.2 hr (Y^{90}), and 57.5 days (Y^{91}). The 16-min component was further resolvable into components of 10-min (Y^{95}) and 19.5-min (Y^{94}) half-life. The decay curve from the 5.00-min bombardment was analyzed through the use of the IBM 704 least-squares program, as were all the yttrium decay curves. The decay curves from the longer bombardments (20 min to 2 hr) yielded β-decay components with half-lives of 19.5 min (Y^{94}), 50 min (Y^{91m}), 3.6 hr (Y^{92}), 10.5 hr (Y^{93}), 64.2 hr (Y^{90}), and 57.5 days (Y^{91}).

Zirconium

The β-decay curve resulting from decay of zirconium isotopes was resolved graphically into components corresponding to half-lives of 17 hr (Zr^{97}) and 65 days (Zr^{95}). The 17-hr component was in equilibrium with the 72-min Nb^{97}. The cross section for the production of Zr^{97} was also measured by using the 3×3-in. NaI crystal and pulse analyzer to observe the γ radiation from decay of Zr^{97}.

Niobium

Least-squares analysis of the niobium β-decay curves yielded components corresponding to half-lives of 52 min (Nb^{98}), 72 min (Nb^{97}), 23 hr (Nb^{96}), 84 hr (Nb^{95m}), and 35 days (Nb^{95}). The Nb^{95} decay was observed additionally on the 3×3-in. crystal by measuring the 760-kev γ radiation.

Molybdenum

The β-decay rate of molybdenum was always measured on shelf 3 of the end-window proportional counter. The β decay always yielded a single component of 66- to 67-hr half-life (Mo^{99}).

Silver

β-proportional counting was used to observe the decay of silver isotopes. IBM least-squares analysis yielded decay components having half-lives of 21 min (Ag^{115}), 3.2 hr (Ag^{112}), 5.3 hr (Ag^{113}), and 7.5 days (Ag^{111}).

Iodine

Yields of iodine isotopes were determined by observing γ radiation on the 3×3-in. and 1.5×1-in. NaI crystals, which were connected to the 100-channel pulse-height analyzer. Peaks were resolved from the total γ spectra by using standards of various energies, and the integrated resolved photopeaks were plotted vs time to give decay curves. Resolution of these decay curves allowed quite certain identification of iodine isotopes (121, 123, 124, 125, 126, 128, 130) as well as allowing determination of their yields.

Cesium

The 3×3-in. NaI crystal and pulse analyzer were used to measure the 670-kev γ radiation of Cs^{132} as well as the 380-kev γ radiation of Cs^{129}.

Barium

The 1.5×1-in. NaI crystal with beryllium window and pulse-height analyzer were used to measure the cesium K x rays from Ba^{131} as well as the xenon K x rays from the decay of the Cs^{131} daughter.